

# DEMOSAICKING ALGORITHM FOR THE FUJIFILM X-TRANS COLOR FILTER ARRAY

*Mina Rafinazari, Eric Dubois\**

University of Ottawa  
School of Electrical Engineering and Computer Science  
Ottawa, Canada

## ABSTRACT

Digital cameras reconstruct a full color image using the information captured by different color sensors (RGB) through a Color Filter Array (CFA). A demosaicking algorithm uses the information of the CFA data to restore a full color array. Demosaicking algorithms reconstruct two unknown color components for a pixel at each spatial location. During this stage, the values of other components will be measured mostly by neighboring pixels' information. Since the Fujifilm X-Trans pattern is one of the more successful CFAs, we attempt to model the demosaicking steps using this pattern and simulate both non-adaptive and adaptive demosaicking schemes. Kodak sample images are used in order to validate and compare different approaches with related previous work.

**Index Terms**— Demosaicking, CFA, Fujifilm, Color image restoration

## 1. INTRODUCTION

Digital cameras are widely used to capture color images by incorporating Color Filter Arrays (CFAs). A CFA is employed to measure three primary colors in a way that each CFA sensor is responsible for capturing only one tristimulus value at a certain pixel location [1]. CFA patterns differ in the number and formation of pixels; the Bayer pattern is the most popular one with a  $2 \times 2$  sensor array consisting two green, one blue and one red pixel [2, 3].

Demosaicking refers to the process of reconstructing an image from incomplete samples. The basic demosaicking scheme relies on simple interpolation between neighboring pixel information and its results are usually poor [4]. In previous research, demosaicking algorithms were analyzed and implemented in the spatial domain and the resulting images were not perfectly reconstructed. Later on, it was demonstrated that the luma and chroma components are reasonably isolated in the frequency domain.

There is a large number of demosaicking schemes employing the Bayer structure in the frequency domain. Some

of these algorithms are proven to produce good results. One of the most recent and well known algorithms which outperforms previous approaches employs Least-Squares optimization [5].

As we know, demosaicking algorithms and CFA design methods are both crucial steps to restore an optimal output, the optimal CFA has been designed in [6] in frequency domain. As different CFA patterns are used in demosaicking algorithms, a comprehensive analysis has been conducted which finally yielded to a methodology to design a better CFA pattern.

We are developing a new demosaicking algorithm using the Fujifilm pattern to enhance the quality of the display with respect to human vision perception. The most popular and simple CFA template is Bayer and we decided to work on other well known patterns and compare the results with Bayer.

We want to study and optimize the reconstruction techniques for various new sampling structures, such as Fujifilm with three color components. This study involves the design of an appropriate demosaicking method and is applied on the Kodak image dataset. Since Fujifilm cameras have been commercially successful, we attempt to model the demosaicking steps using the X-Trans Fujifilm pattern and simulate non-adaptive and adaptive demosaicking algorithms in Matlab software. A detailed optimization of filter parameters and the region of support will be addressed.

## 2. METHOD

In this paper we implement demosaicking algorithms related to the Fujifilm X-Trans CFA pattern. The Fujifilm CFA pattern is a  $6 \times 6$  template containing 20 green pixels, 8 blue and 8 red as we can see in Figure 1. The number of green pixels is more than the total number of blue and green pixels. This template provides a higher degree of randomness with an array of  $6 \times 6$  pixel units. According to the manufacturer, without using an optical low-pass filter, moiré and false colors are eliminated while realizing high resolution. Analysis of this pattern is more complicated than for the Bayer pattern due to the large number of sensors in one period of the CFA [7].

\*This work was funded by NSERC.

The CFA signal is sampled on lattice  $\Lambda = \mathbb{Z}^2$  with reciprocal lattice  $\Lambda^* = \mathbb{Z}^2$ .

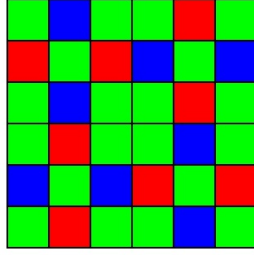


Fig. 1: Fujifilm CFA pattern

Although the pattern is generally viewed as  $6 \times 6$ , it is in fact  $3 \times 6$  with periodicity is given by a hexagonal lattice. A lattice and its corresponding reciprocal lattice to represent the periodicity of the CFA pattern can be given by:

$$V_{\Gamma} = \begin{bmatrix} 6 & 3 \\ 0 & 3 \end{bmatrix}, \quad V_{\Gamma^*} = \begin{bmatrix} \frac{1}{6} & 0 \\ -\frac{1}{3} & \frac{1}{3} \end{bmatrix} \quad (1)$$

The analysis of this CFA can be carried out using the general theory described in [8], to which the reader should refer for more details.

According to the analysis, the CFA signal can be represented as a sum of modulated chroma components plus a baseband luma component. The CFA signal is given by

$$f_{CFA}[\mathbf{x}] = \sum_{i=1}^K q_i[\mathbf{x}] \exp(j2\pi(\mathbf{x} \cdot \mathbf{d}_i)) \quad \text{where } K = 18, \quad (2)$$

where the  $\mathbf{d}_i$  are representatives of cosets of  $\Lambda^*$  in  $\Gamma^*$ . They are specified by the columns of a  $2 \times K$  matrix  $D$ , which for this pattern is.

$$D = \begin{bmatrix} 0 & \frac{2}{6} & -\frac{2}{6} & \frac{1}{6} & -\frac{1}{6} & \frac{2}{6} & -\frac{2}{6} & \frac{1}{6} & -\frac{1}{6} \\ 0 & 0 & 0 & \frac{1}{6} & -\frac{1}{6} & \frac{2}{6} & -\frac{2}{6} & -\frac{1}{6} & \frac{1}{6} \\ 0 & 0 & \frac{2}{6} & -\frac{2}{6} & \frac{3}{6} & -\frac{1}{6} & \frac{3}{6} & \frac{1}{6} & \frac{3}{6} \\ -\frac{2}{6} & \frac{2}{6} & -\frac{2}{6} & \frac{2}{6} & -\frac{1}{6} & \frac{3}{6} & \frac{1}{6} & \frac{3}{6} & \frac{3}{6} \end{bmatrix} \quad (3)$$

The luma and chroma components are obtained from the original RGB components by

$$\mathbf{q}[\mathbf{x}] = \mathbf{M}\mathbf{f}[\mathbf{x}] \quad (4)$$

$$\mathbf{f} = [f_1, f_2, f_3]^T = [R, G, B]^T \quad \text{and} \quad \mathbf{q} = [q_1, q_2, \dots, q_{18}]^T \quad (5)$$

The matrix  $M$  has been calculated based on the method described in [8] for the Bayer and some other known patterns and we extend it here to the Fujifilm pattern. The following matrix shows the calculated matrix  $M$  for 18 components.

Note that only 13 components are nonzero.

$$M = \begin{bmatrix} 0.2222 & 0.5556 & 0.2222 \\ -0.0278 - 0.0481i & 0.0556 + 0.0962i & -0.0278 - 0.0481i \\ -0.0278 + 0.0481i & 0.0556 - 0.0962i & -0.0278 + 0.0481i \\ 0 & 0 & 0 \\ 0 & 0 & 0 \\ 0.0556 - 0.0962i & -0.1111 + 0.1925i & 0.0556 - 0.0962i \\ 0.0556 + 0.0962i & -0.1111 - 0.1925i & 0.0556 + 0.0962i \\ 0 & 0 & 0 \\ 0 & 0 & 0 \\ -0.0278 + 0.0481i & 0.0556 - 0.0962i & -0.0278 + 0.0481i \\ -0.0278 - 0.0481i & 0.0556 + 0.0962i & -0.0278 - 0.0481i \\ -0.1111 & 0.2222 & -0.1111 \\ -0.1111 & 0.2222 & -0.1111 \\ 0.0833 + 0.1443i & 0 & -0.0833 - 0.1443i \\ -0.0833 - 0.1443i & 0 & 0.0833 + 0.1443i \\ 0.0833 - 0.1443i & 0 & -0.0833 + 0.1443i \\ -0.0833 + 0.1443i & 0 & 0.0833 - 0.1443i \\ 0 & 0 & 0 \end{bmatrix} \quad (6)$$

In the frequency domain, using the standard modulation property of the Fourier transform, we find

$$F_{CFA}(\mathbf{u}) = \sum_{i=1}^{18} Q_i(\mathbf{u} - \mathbf{d}_i) \quad \text{Where } Q_i(\mathbf{u}) \triangleq \mathcal{F}\{q_i[\mathbf{x}]\} \quad (7)$$

Figure 2 shows the position of luma and chroma components in one unit cell of  $\Lambda^*$ . Basic frequency-domain

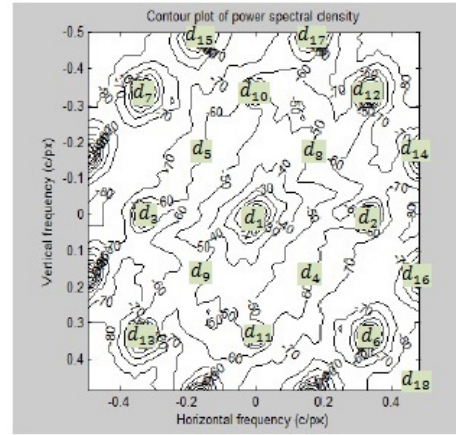


Fig. 2: Luma- Chroma position

demaasking involves extracting the 17 chroma components with bandpass filters separately, demodulating them to baseband and reconstructing the estimated RGB signal based on these signals with

$$\hat{\mathbf{f}}[\mathbf{x}] = \mathbf{M}^{\dagger} \hat{\mathbf{q}}[\mathbf{x}] \quad (8)$$

where  $\mathbf{M}^{\dagger}$  is the pseudo inverse matrix of  $\mathbf{M}$ . In the filtering stage, three different baseband Gaussian filters have been designed to filter different chromas by modulating them to the different band center frequencies. The first filter extracted  $q_2, q_3, q_{10}$  and  $q_{11}$ . The second one has been used

for  $q_6, q_7, q_{12}$  and  $q_{13}$  and the last one extract  $q_{14}, q_{15}, q_{16}$  and  $q_{17}$ .

The Luma component will be extracted as follows:

$$\hat{q}_1[\mathbf{x}] = f_{CFA}[\mathbf{x}] - \sum_{i=2}^{18} \hat{q}_i \exp(j2\pi(\mathbf{x} \cdot \mathbf{d}_i)). \quad (9)$$

Although we model the whole system for 18 components, there are 5 components with  $q_i[\mathbf{x}]$  equal to zero. These are related to  $d_4, d_5, d_8, d_9$  and  $d_{18}$ .

Based on the dependence of different chroma components we can categorize all 18 component into 5 groups and estimate the rest of the components based on them. The following equations show the relations between the 13 nonzero components.

$$p_1(\mathbf{x}) \triangleq q_1(\mathbf{x}) \quad \text{Luma} \quad (10)$$

$$p_2(\mathbf{x}) \triangleq q_{12}(\mathbf{x}) = q_{13}(\mathbf{x}) \quad (11)$$

$$p_3(\mathbf{x}) \triangleq q_2(\mathbf{x}) = q_3^*(\mathbf{x}) = q_{10}^*(\mathbf{x}) = q_{11}(\mathbf{x}) \quad (12)$$

$$p_4(\mathbf{x}) \triangleq q_6(\mathbf{x}) = q_7^*(\mathbf{x}) \quad (13)$$

$$p_5(\mathbf{x}) \triangleq q_{14}(\mathbf{x}) = q_{16}^*(\mathbf{x}) = -q_{15}(\mathbf{x}) = -q_{17}^*(\mathbf{x}) \quad (14)$$

By inspecting the values of matrix  $M$ , the values of some components can be retrieved based on the others. The following equations show further relations between different components:

$$q_{12}(\mathbf{x}) = q_{13}(\mathbf{x}) = -(q_6(\mathbf{x}) + q_7(\mathbf{x})) \quad (15)$$

$$q_6(\mathbf{x}) = -(q_2(\mathbf{x}) + q_3(\mathbf{x})) + j(q_2(\mathbf{x}) - q_3(\mathbf{x})) \quad (16)$$

Thus we can calculate  $p_2, p_3$  and  $p_4$  using the real and imaginary part of one of them. Since the value of  $p_2$  is real, we need to have either  $p_3$  or  $p_4$  to find the rest.

$$p_2(\mathbf{x}) = -2\text{Re}\{p_4(\mathbf{x})\} \quad (17)$$

$$p_4(\mathbf{x}) = -2\text{Re}\{p_3(\mathbf{x})\} + j2\text{Im}\{p_3(\mathbf{x})\} \equiv 2p_3^*(\mathbf{x}) \quad (18)$$

We can conclude that all the first 8 chroma components can be calculated based on any of these components. Thus we are able to estimate some of the chromas which have more interference with Luma based on the other components that are further from Luma.

In summary we have  $p_1$  as luma,  $p_5$  as the first chroma and one of  $p_2, p_3$  and  $p_4$  as the second chrominance. In the adaptive method, weights will be assigned to the chromas selectively. The more accurately reconstructed chroma in each group receives a higher weight and the other chroma component will be updated sequentially. The new estimated chromas improve the luma estimation as well.

The adaptive algorithm tries to update the chroma components which are closer to the luma such as  $q_2, q_3, q_{10}$  and  $q_{11}$ , since they have more crosstalk with luma. Based on equation 12, we need to update one of these chromas such as  $q_2$  using a weighted form of the rest. The updated  $q_2$  will help us to reconstruct the enhanced  $q_3, q_{10}, q_{11}$  and luma. The nonadaptive algorithm extracts the chromas using the Gaussian filters and simply reconstructs the RGB image using the extracted chromas.

In comparing demosaicking algorithms using Fujifilm and Bayer patterns, we note that there were also three selected independent components in Bayer.

### 3. RESULTS AND DISCUSSION

The Fujifilm pattern is interesting because of its specific structure and the different number of RGB pixels. Since it is commercially and experimentally successful and also there was a lack of research in the demosaicking algorithm using Fujifilm pattern we introduce a demosaicking method using Fujifilm pattern characteristics and implement it in Matlab environment. This research reconstructs the 24 Kodak images using Fujifilm pattern to compare them with the previous patterns.

Table 1 shows the PSNR comparison between the least-squares luma-chroma demultiplexing (LSLCD) method using Bayer, adaptive and nonadaptive demosaicking scheme using X-Trans pattern for some sample images as well as the average PSNR over 24 kodak images.

The table shows that the proposed adaptive demosaicking scheme using the Fujifilm pattern gives us a comparable set of PSNR with the LSLCD demosaicking scheme using Bayer pattern. On the other hand, the visual results show improvement in the reconstructed details and its colors.

Figure 3 and 4 show the horizontal, vertical and diagonal details in the reconstructed images using Bayer and Fujifilm pattern. The visual results prove the X-trans pattern gives less false colors than Bayer pattern on these details.

Image number	LSLCD method	Fujifilm(Adaptive demosaicking)	Fujifilm(Non Adaptive demosaicking)
01	37.9	36.2	32.09
02	39.9	38.8	35.7
03	35.3	35.5	33.1
04	38.7	37.08	34.8
05	34.2	32.9	30.9
Average over 24 images	39.8	36.5	34.8

**Table 1:** PSNR of some sample images using Bayer and X-Trans(Adaptive and Non-adaptive) and the average PSNR over 24 Kodak images



(a) Original image



(b) Reconstructed using X-Trans

(c) Reconstructed using Bayer

**Fig. 3:** Comparison between The new method using X-Trans and LSLCD method using Bayer



(a) Original image



(b) Reconstructed using X-Trans

(c) Reconstructed using Bayer

**Fig. 4:** Comparison between The new method using X-Trans and LSLCD method using Bayer

#### 4. CONCLUSION

This research addressed a new demosaicking algorithm for the X-Trans pattern. Since the pattern is quite different and more complex than the other patterns a new demosaicking

algorithm has been proposed. Based on the new adaptive method using the X-Trans template, the quality of reconstructed images is enhanced and the false colors decreased compared to the previous demosaicking method. Then, future work will involve improving the filter design using the least-square methodology, as in [4].

#### 5. REFERENCES

- [1] K. Hirakawa, X. Li, and P.J. Wolfe, "A framework for wavelet-based analysis and processing of color filter array images with applications to denoising and demosaicing," in *2007 IEEE International Conference on Acoustics, Speech and Signal Processing (ICASSP 2007)*, April 2007, vol. 1, pp. 597–600.
- [2] O. Losson, L. Macaire, and Y. Yang, "Comparison of Color Demosaicing Methods", vol. 162 of *Advances in Imaging and Electron Physics*, chapter 5, pp. 173 – 265, Elsevier, 2010.
- [3] X. Li, B. Gunturk, and L. Zhang, "Image demosaicing: a systematic survey," *SPIE 6822, Visual Communications and Image Processing*, January 2008.
- [4] B. Leung, G. Jeon, and E. Dubois, "Least-squares luma-chroma demultiplexing algorithm for bayer demosaicking," *IEEE Transactions on Image Processing*, vol. 20, no. 7, pp. 1885–1894, July 2011.
- [5] E. Dubois, "Frequency-domain methods for demosaicking of bayer-sampled color images," *Signal Processing Letters, IEEE*, vol. 12, no. 12, pp. 847–850, Dec 2005.
- [6] P. Hao, Y. Li, Z. Lin, and E. Dubois, "A geometric method for optimal design of color filter arrays," *IEEE Transactions on Image Processing*, vol. 20, no. 3, pp. 709–722, March 2011.
- [7] "Fujifilm x-pro1," <http://www.fujifilmusa.com/products/digital-cameras/x/fujifilm-x-pro1/features>.
- [8] E. Dubois, "Color filter array sampling of color images," in *Single-Sensor Imaging Methods and Applications for Digital Cameras*, Rastislav Lukac, Ed., chapter 7, pp. 183–212. CRC Press, 2008.